

**Deformation behavior observation of slow-rate compression and tensile
after compression in a CoCrNiSi medium entropy alloy via in-situ
deformation transmission electron microscope**

Cheng-Ling Tai ^a, II Seiichiro ^b, Takahito Ohmura ^b, Jer-Ren Yang ^{a,*}

^a Department of Materials Science and Engineering, National Taiwan University, Taipei 10617, Taiwan.

^b National Institute for Materials Science, 1-2-1 Sengen, Tsukuba, Ibaraki 305-0047, Japan

Abstract

CoCrNi medium-entropy alloys exhibit exceptional strength and ductility at low temperatures due to the formation of deformation twins. However, their strength at room temperature remains insufficient. The addition of Si serves the dual purpose of achieving lightweighting and enhancing solid solution strengthening while reducing stack fault energy. Additionally, controlled compression of specific materials can further enhance subsequent tensile strength. This study investigates the deformation behavior of a lightweight CoCrNiSi medium-entropy alloy through in-situ deformation transmission electron microscopy (in-situ deformation TEM), utilizing nano-indentation for slow compression and subsequent tensile testing of nano-pillars. Observations are conducted under a two-beam condition with the $g = [110]$ direction to minimize displayed dislocations by half and alleviate issues associated with excessive dislocation hindering observation. Results indicate that, during slow compression deformation of CoCrNiSi, stacking faults and dislocations form in the early stages, with a subsequent formation of a small number of deformation twins, impeding dislocation movement. In subsequent tensile experiments, a significant number of deformation twins are observed. This suggests that pre-compression to induce deformation twins, followed by a tensile test, expedites the attainment of critical shear stress for deformation twins, leading to a material with higher strength. This study provides direct evidence of the microstructural deformation mechanism in a CoCrNiSi medium-entropy alloy for lightweight applications. The approach of slow compression followed by tensile testing complements simulation calculations, addressing their limitation of lacking direct evidence of deformation behavior.

Key words: CoCrNi medium entropy alloy; Si addition; In-situ deformation transmission electron microscope; Deformation twin; Tensile after compression

Introduction

In recent years, there has been rapid development in the field of single-phase high-entropy alloys (HEAs) due to their exceptional mechanical properties, including high strength and ductility, particularly at low temperatures [1-3]. High-entropy alloys are characterized by compositions comprising more than five principal elements, each ranging from 5 at. % to 35 at. %, resulting in four key effects: (1) the high-entropy effect, (2) slow atomic diffusion effect, (3) severe lattice distortion effect, and (4) cocktail effect [4-6]. These effects make high-entropy alloys more inclined to form simple solid solution structures rather than intermetallic compounds. Among the renowned high-entropy alloys is the Cantor alloy [7] (FeCoNiCrMn). Derived from the Cantor alloy, the ternary CoCrNi medium entropy alloy (MEA) [8] was developed, exhibiting superior mechanical properties.

Previous studies [9, 10] have demonstrated that the judicious addition of silicon to isotropic CoCrNi MEA significantly enhances overall mechanical properties, including yield strength, maximum tensile strength, and total elongation. This improvement is attributed not only to the solid solution strengthening effect but also to the reduction of superposition difference energy (SFE) following the addition of silicon. In low SFE CoCrNi MEA with silicon, the formation of deformation twin and hexagonal closely packed structures (HCP) during deformation becomes more feasible, substantially increasing tensile strength [11]. Moreover, various studies have revealed that in different alloys such as stainless steels [12, 13] and magnesium alloys [14], the buckling strength and tensile strength can be significantly enhanced through pre-compression and re-stretching. In a particular study [13], the yield strength and work-hardening rate of Mn18Cr18N austenite stainless steel were notably improved by subjecting it to a pre-compression of 30%, leading to the formation of a deformation twin, followed by stretching, thereby enhancing the material's strength. In this study, the deformation behavior of CoCrNiSi0.3 MEA has been investigated through in-situ deformation transmission electron microscopy (TEM) as direct evidence of its behavior after slow compression and stretching.

Experimental Procedure:

The study employed CoCrNiSi MEA, and the microstructural changes after compression and stretching were examined. In-situ deformation of CoCrNiSi MEA nano-pillars in TEM (JEOL ARM300F) was conducted. The material was homogenized at 1100 °C for 2 days to eliminate dendrites formed during the casting process. A specific direction ([110] direction) was selected as the deformation direction using scanning electron microscope (SEM) electron back scatter diffraction (EBSD) technique, as shown in Fig. 1a. Subsequently, a specific direction ([1-10] direction) was chosen as the observation direction using OIM software. In-situ deformation TEM samples were prepared by focused ion beam (FIB; JEM-9310FIB) along the [1-10] direction, forming a nanopillar with a width of 300 nm, a length of 600 nm, and a thickness of about 100 nm, as illustrated in Fig. 1b and Fig. 1c. Compression and tensile tests were conducted under two-beam conditions (Fig. 1d), with a strain rate of approximately 10^{-3} s⁻¹.

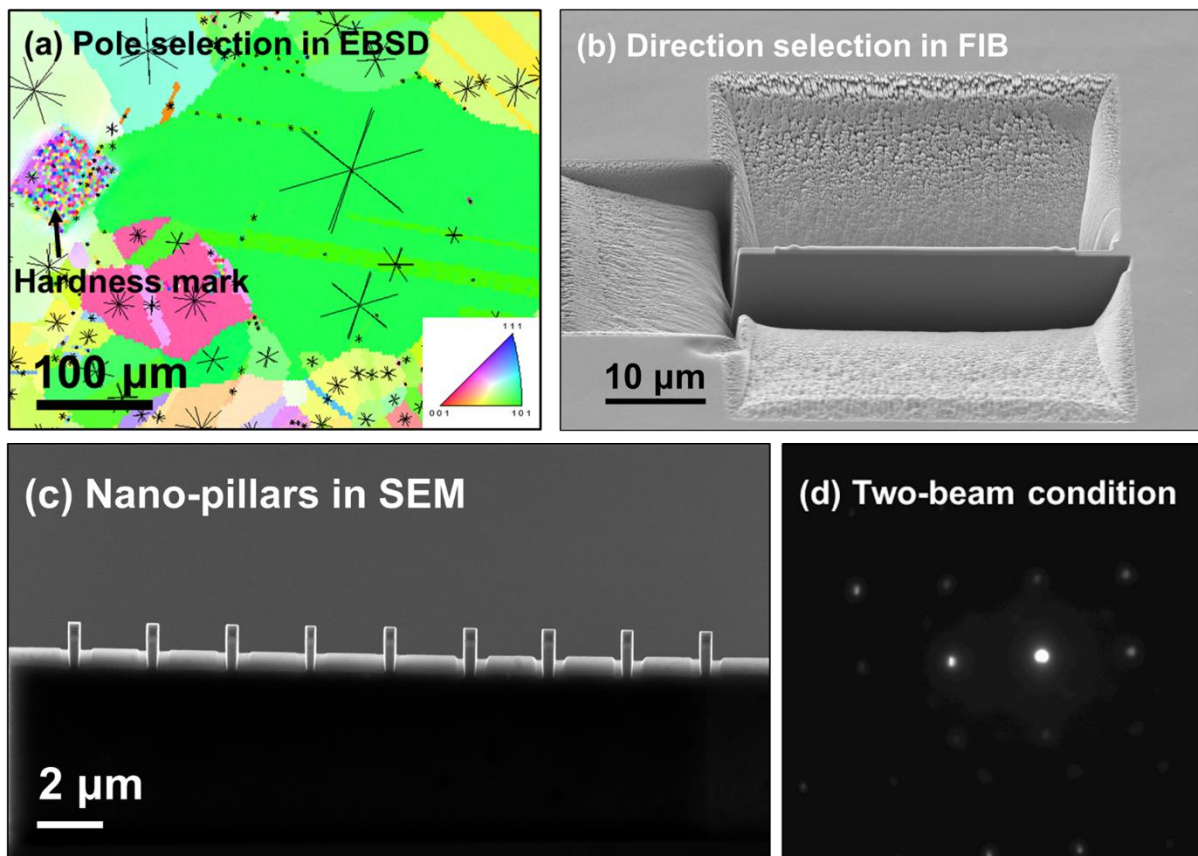


Fig. 1. (a) Selecting the deformation direction under EBSD and the observation direction by OIM software. (b) A plate of the selected direction was cut by FIB. (c) SEM image of the nanopillars. (d) Observation under two-beam condition.

Results and discussion

3.1. Slow-rate compression test

In this study, the compression experiment is conducted along the $[110]$ direction, and TEM images of the nano-pillars are obtained under the $g = [110]$ two-beam condition. This observation condition reduces the displayed dislocations by half, preventing an excessive number of dislocations that might overlook the time of deformation twin formation. Fig. 2a illustrates the corresponding stress-strain curve, and Fig. 2b displays the nano-pillar before deformation. Upon reaching a deformation of 3.5%, the yield strength is attained, and dislocations gradually emerge, as shown in Figure 2c. The strength increases steadily until surpassing the yield strength, causing a sudden drop. This phenomenon occurs not due to material softening but because multiple dislocations slip out of the specimen through the boundary simultaneously, creating a gap between the nano-pillar and the nano-indenter. The subsequent contact between the two leads to a renewed increase in strength. The yield strength after elastic deformation is reached at 2.11 GPa.

As deformation progresses, in addition to the initial slip bands, dislocations move out of the boundary through formed slip bands in the corner area, making it challenging for dislocations to accumulate and preventing the formation of entangled dislocations. The deformation mechanism continues to be dominated by slip bands, but deformation twins are already observed in the yellow-framed area (Fig. 2d), contributing to the sustained strength of the continuously formed slip bands. With continued force application, deformation twins form throughout the specimen except for the corner area (Fig. 2e), where the addition of Si reduces stacking differential energy, hindering dislocation movement. This increased difficulty allows them to accumulate and more likely reach the critical deformation twin shear stress value, shifting the deformation mechanism to a twin mechanism. Subsequently, deformation twin formed on another 111 plane in the corner slip area is observed, preventing slipping and further enhancing strength (Fig. 2f). The intersection of Figs 2g and 2h exhibits the same morphology, signifying a cessation of deformation by slipping. As deformation intensifies, more deformation

twin form, with two sets of deformation twin staggered, impeding the slip deformation of the differential rows and increasing strength. However, after reaching a certain deformation extent, excessive defects make the specimen resistant to distortion, resulting in no further increase in strength, as depicted in Fig. 2h.

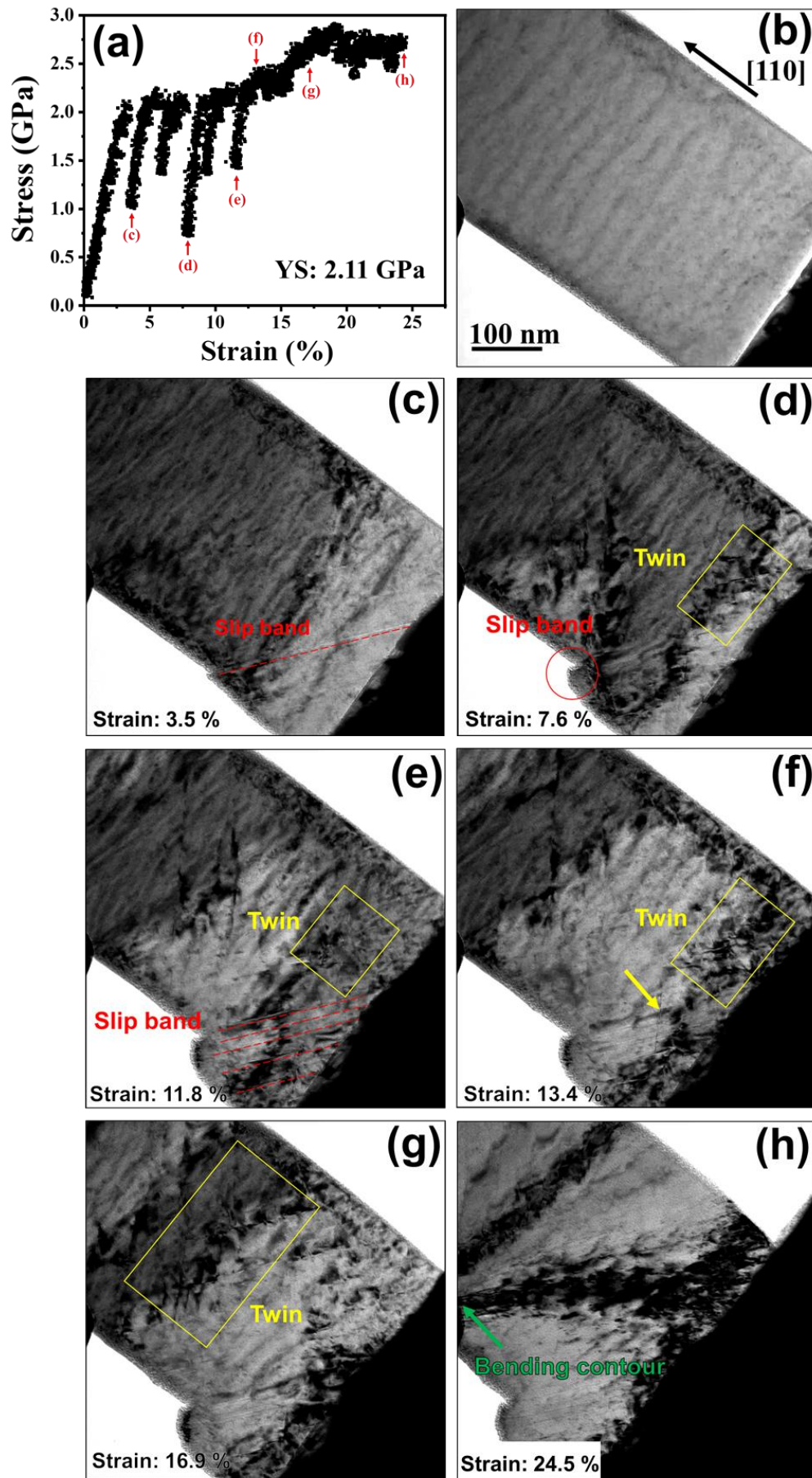


Fig. 2. TEM images of the deformation of the nano-pillar. (a) Stress strain curve. (b)-(h) Evolutions of the morphology and microstructures of the nano-pillar during compression.

3.2. Stretching after compression

Fig. 3a presents the TEM image of the nano-pillar before compression at $g = [110]$ under two-beam condition. Upon reaching a 4.0% deformation, the yield strength is achieved, and dislocations gradually emerge, as depicted in Fig. 3b. The strength steadily increases until reaching the buckling intensity, where it suddenly drops and then rises again. Notably, at a compression of 6.3%, distinct stacking is observed, and some deformation twins form in the heavily deformed area, as shown in Fig. 3c. In Fig. 4a, the image displays the nano-pillar after compression, leading to the formation of deformation twins. With a slight stretch, numerous deformation twins swiftly generate in the base, indicating an immediate attainment of the critical deformation twin shear stress value, intersecting with each other. This intersecting is favorable for halting the slip of dislocations, enhancing strength, as illustrated in Fig. 4b. Progressing with slow stretching, more deformation twins form in the matrix. The contrast of black color indicates the concentration of dislocations and the formation of additional strain field, as seen in Fig. 4c. This intensified deformation and the presence of deformation twins effectively prevent dislocation movement, further improving the material's strength.

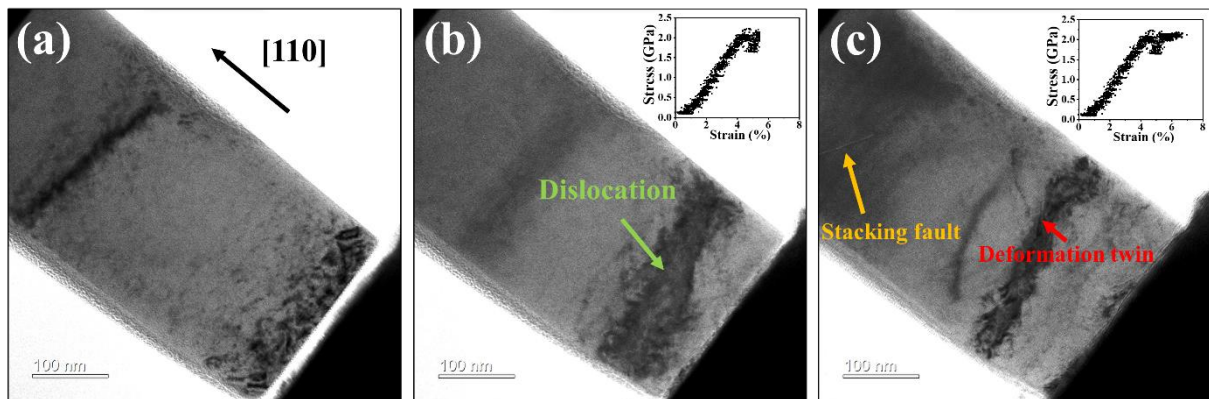


Fig. 3. TEM images of the nano-pillar. (a) Nano-pillar before compression. (b) Nano-pillar with 4.0% deformation. (c) Nano-pillar with 6.3% deformation.

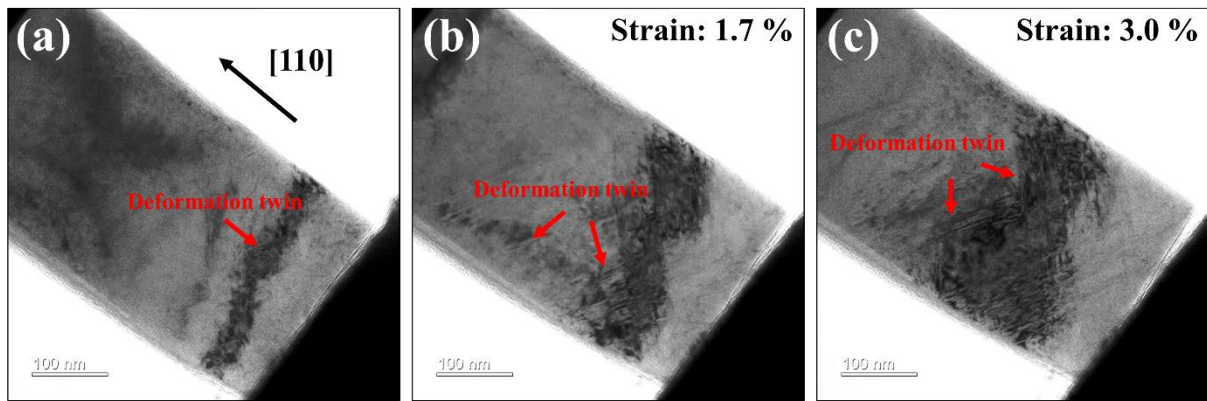


Fig. 4. TEM images of: (a) Nano-pillar before stretching. (b) Nano-pillar after 1.7 % and (c) after 3.0% stretching.

Fig. 3 and Fig. 4 illustrate the microstructural evolutions resulting from slow stretching, nuances that might go unnoticed under two-beam conditions. To delve into the microstructural alterations following slow stretching, the $[110]$ zone axis was employed. In Fig. 5a, a substantial number of deformation twins are evident in the stretched test specimen, forming an angle of 70.52° to each other, resembling the effects of grain refinement [15]. The close blocks are depicted in detail in Fig. 5c. Examining Fig. 5b, streaks on the two 111 planes are observable, stemming from deformation twins growing on the $\{111\}$ plane, albeit in small and insufficient numbers. Moreover, a higher density of deformation twins is noted at the specimen's top due to non-uniform deformation during compression, where a significant accumulation of dislocations and a limited number of deformation twins occur. This accumulation facilitates the swift attainment of the critical deformation twin shear value during subsequent tensile deformation, shifting the deformation mechanism from dislocation to a twin mechanism. As deformation intensifies, a substantial accumulation of dislocations occurs along the boundary of the deformation twins, showcased in Fig. 5a, underscoring the deformation twin's capability to impede dislocations, significantly fortifying the material.

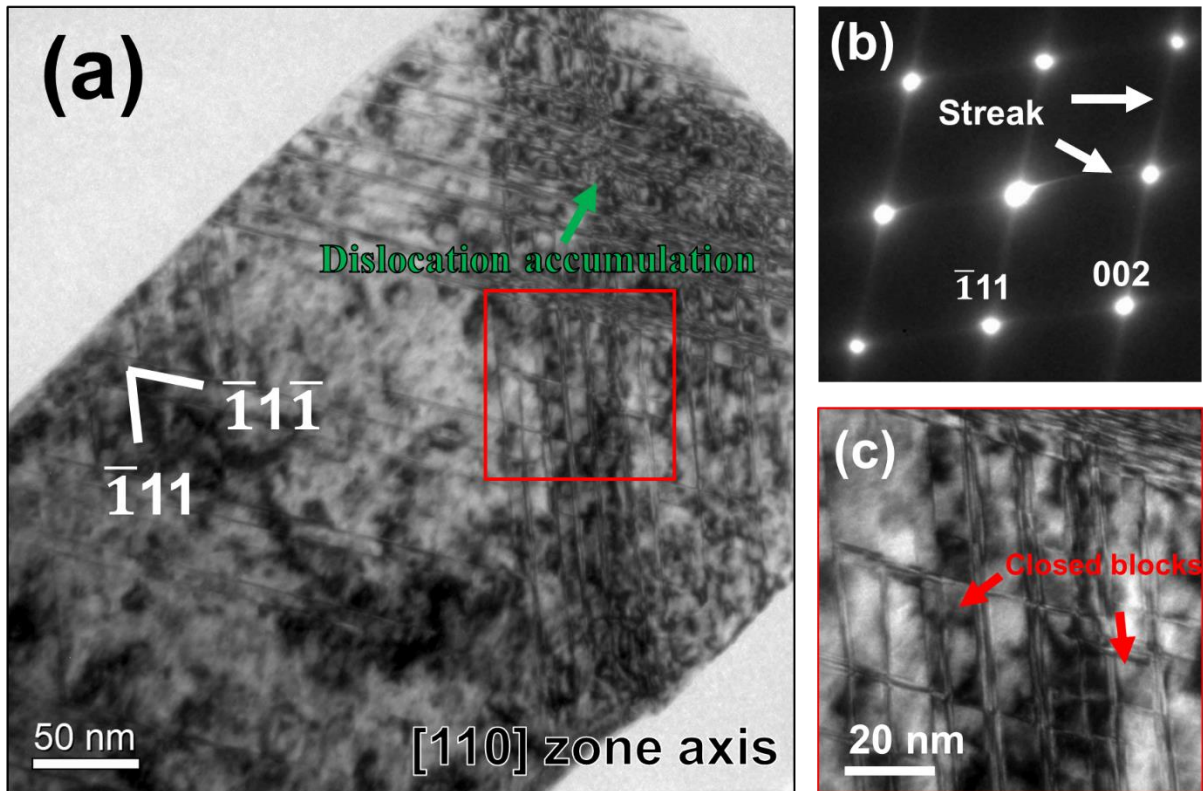


Fig. 5. (a) The TEM image of the stretched nano-pillar observed on the along [110]. (b) The diffraction pattern of Fig. 5a. (c) Enlarged view of the red-square area in Fig. 5a, which has formed a dynamic grain refinement effect.

Conclusions

In this study, we examined the deformation behavior of CoCrNiSi under slow compression using an in-situ deformation transmission electron microscope. The results reveal that once dislocations aggregate in materials with low stacking energy, a transition occurs from dislocation slip to a deformation mechanism based on deformation twins, effectively enhancing material strength. Moreover, pre-compressing generates a small quantity of deformation twins before stretching accelerating their formation during tensile deformation. The resultant large number of deformation twins effectively hinders differential slip, consequently increasing the material's work-hardening rate. Additionally, since the top of the nano-pillar experiences more intense deformation during compression, it accelerates deformation twin formation during subsequent stretching. This indicates that the magnitude of pre-compression deformation and the introduced defect count directly influence material deformation behavior and mechanical properties during subsequent stretching. Utilizing the in-situ deformation transmission electron microscope can clearly comprehend material deformation behavior changes. For materials with

low stacking fault energy, the timing of deformation twin formation can be observed, which suggests the degrees of introduction of pre-distortion to achieve the desired mechanical properties for the material.

Reference

- [1] S. Bajpai, B.E. MacDonald, T.J. Rupert, H. Hahn, E.J. Lavernia, D. Apelian, Recent progress in the CoCrNi alloy system, *Materialia* (2022) 101476.
- [2] Y. Zhang, T.T. Zuo, Z. Tang, M.C. Gao, K.A. Dahmen, P.K. Liaw, Z.P. Lu, Microstructures and properties of high-entropy alloys, *Progress in materials science* 61 (2014) 1-93.
- [3] G. Laplanche, A. Kostka, O. Horst, G. Eggeler, E. George, Microstructure evolution and critical stress for twinning in the CrMnFeCoNi high-entropy alloy, *Acta Materialia* 118 (2016) 152-163.
- [4] J.W. Yeh, S.K. Chen, S.J. Lin, J.Y. Gan, T.S. Chin, T.T. Shun, C.H. Tsau, S.Y. Chang, Nanostructured high-entropy alloys with multiple principal elements: novel alloy design concepts and outcomes, *Advanced engineering materials* 6(5) (2004) 299-303.
- [5] Y. Zhang, Y.J. Zhou, J.P. Lin, G.L. Chen, P.K. Liaw, Solid-solution phase formation rules for multi-component alloys, *Advanced engineering materials* 10(6) (2008) 534-538.
- [6] X. Yang, Y. Zhang, Prediction of high-entropy stabilized solid-solution in multi-component alloys, *Materials Chemistry and Physics* 132(2-3) (2012) 233-238.
- [7] B. Cantor, I. Chang, P. Knight, A. Vincent, Microstructural development in equiatomic multicomponent alloys, *Materials Science and Engineering: A* 375 (2004) 213-218.
- [8] B. Gludovatz, A. Hohenwarter, K.V. Thurston, H. Bei, Z. Wu, E.P. George, R.O. Ritchie, Exceptional damage-tolerance of a medium-entropy alloy CrCoNi at cryogenic temperatures, *Nature communications* 7(1) (2016) 10602.
- [9] J. Kumar, A. Linda, M. Sadhasivam, K. Pradeep, N. Gurao, K. Biswas, The effect of Si addition on the structure and mechanical properties of equiatomic CoCrFeMnNi high entropy alloy by experiment and simulation, *Materialia* 27 (2023) 101707.

- [10] Z. Li, L. Chen, P. Fu, H. Su, P. Dai, Q. Tang, The effect of Si addition on the heterogeneous grain structure and mechanical properties of CrCoNi medium entropy alloy, *Materials Science and Engineering: A* 852 (2022) 143655.
- [11] H. Chang, T. Zhang, S. Ma, D. Zhao, R. Xiong, T. Wang, Z. Li, Z. Wang, Novel Si-added CrCoNi medium entropy alloys achieving the breakthrough of strength-ductility trade-off, *Materials & Design* 197 (2021) 109202.
- [12] F. LI, H. ZHANG, W. HE, H. CHEN, H. GUO, Compression and tensile consecutive deformation behavior of Mn18Cr18N austenite stainless steel, *Acta Metall Sin* 52(8) (2016) 956-964.
- [13] J.-H. Shin, J.-W. Lee, Effects of twin intersection on the tensile behavior in high nitrogen austenitic stainless steel, *Materials characterization* 91 (2014) 19-25.
- [14] S. Yin, H. Yang, S. Li, S. Wu, F. Yang, Cyclic deformation behavior of as-extruded Mg–3% Al–1% Zn, *Scripta Materialia* 58(9) (2008) 751-754.
- [15] T.-F. Chung, P.-J. Chen, C.-L. Tai, P.-H. Chiu, Y.-S. Lin, C.-N. Hsiao, C.-Y. Chen, S.-H. Wang, J.-W. Yeh, W.-S. Lee, Investigation of nanotwins in the bimodal-structured Fe₂₂Co₂₂Ni₂₀Cr₂₂Mn₁₄ alloy subjected to high-strain-rate deformation at cryogenic temperatures, *Materials Characterization* 170 (2020) 110667.